Supporting Information

Unraveling Antisolvent Dripping Delay Effect on Stranski-Krastanov Growth of $CH_3NH_3PbBr_3$ Thin Films with Improved Optical and Electrical Properties

Jitendra Kumar [a,‖], *Ramesh Kumar* [a,‖], *Kyle Frohna*[b], *Dhanashree Moghe*[c], *Samuel D. Stranks*[b], *Monojit Bag*[†,*]

a Advanced Research in Electrochemical Impedance Spectroscopy, Indian Institute of Technology Roorkee, Roorkee 247667, India

b Cavendish Laboratory University of Cambridge, Cambridge, CB3 0HE, UK

c Department of Physics, Indian Institute of Technology Bombay, Mumbai 400076, India

Email: monojit.bag@ph.iitr.ac.in

‖ Equal contribution

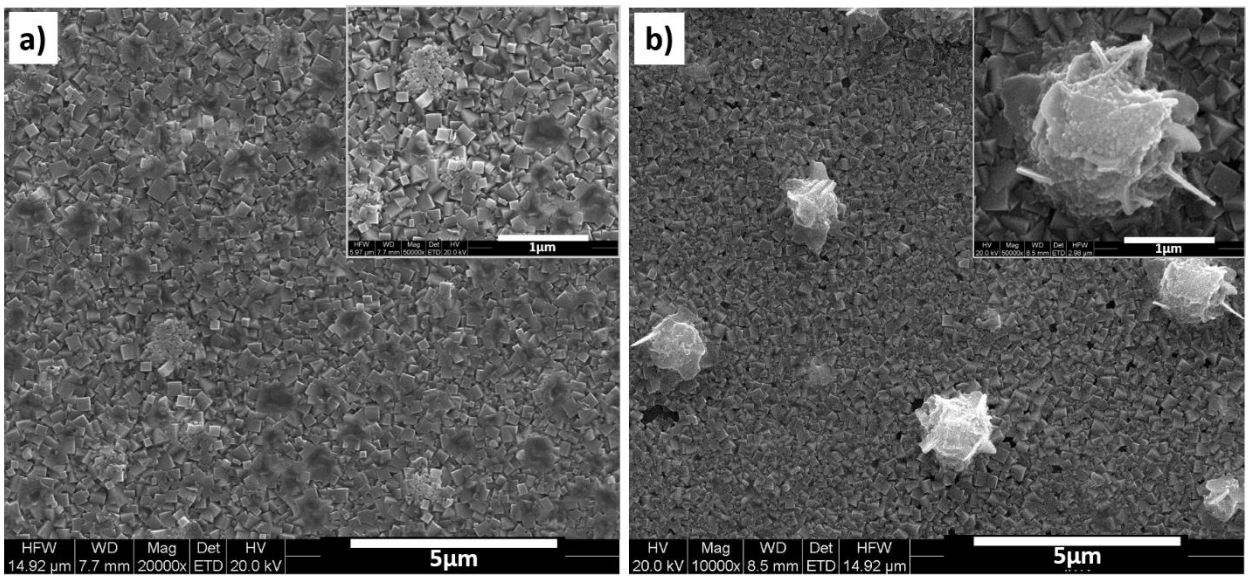

Figure S1. Field emission scanning electron microscope (FESEM) images of (a) smooth film (b) Formation of micro-islands over a compact perovskite film. The film (textured film) shows the presence of smaller (~20-40 nm) crystals at the micro-island site whereas comparatively larger (~300nm) crystals away from the micro-islands. The regions of textured film that are away from the micro-island could be considered as smooth film.

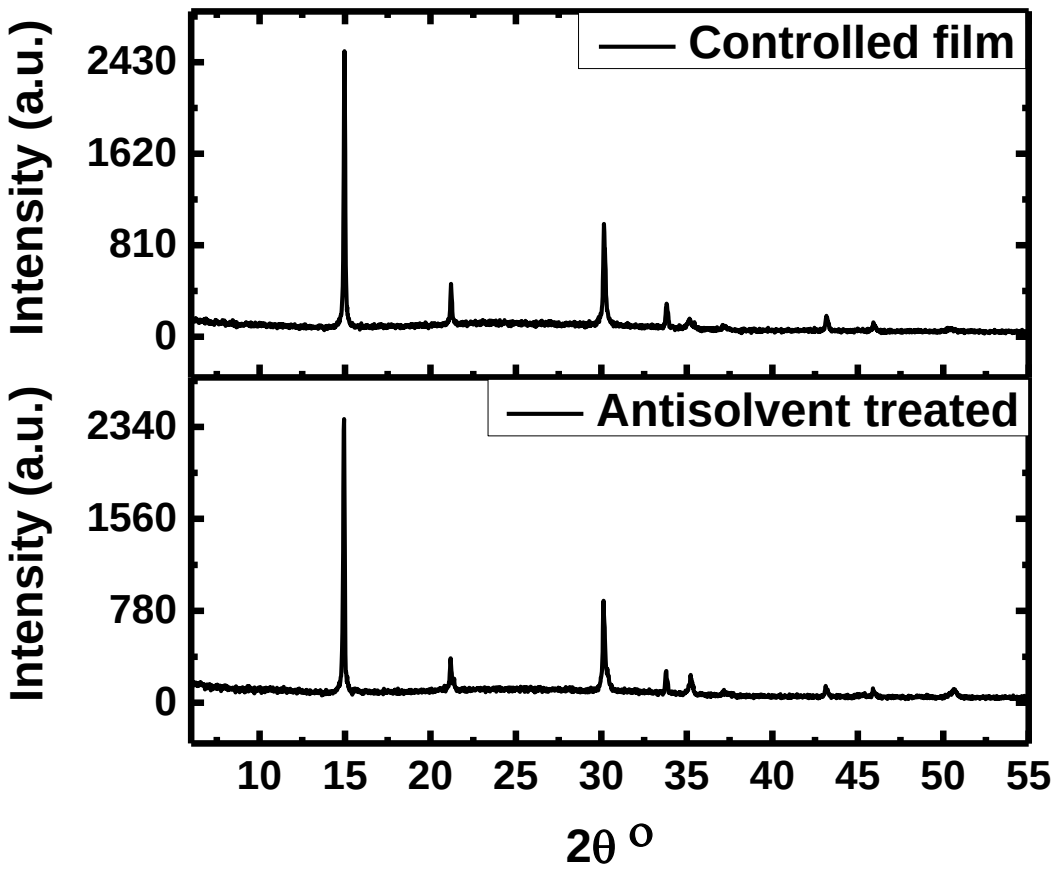

Figure S2. XRD pattern for the controlled and anti-solvent treated film.

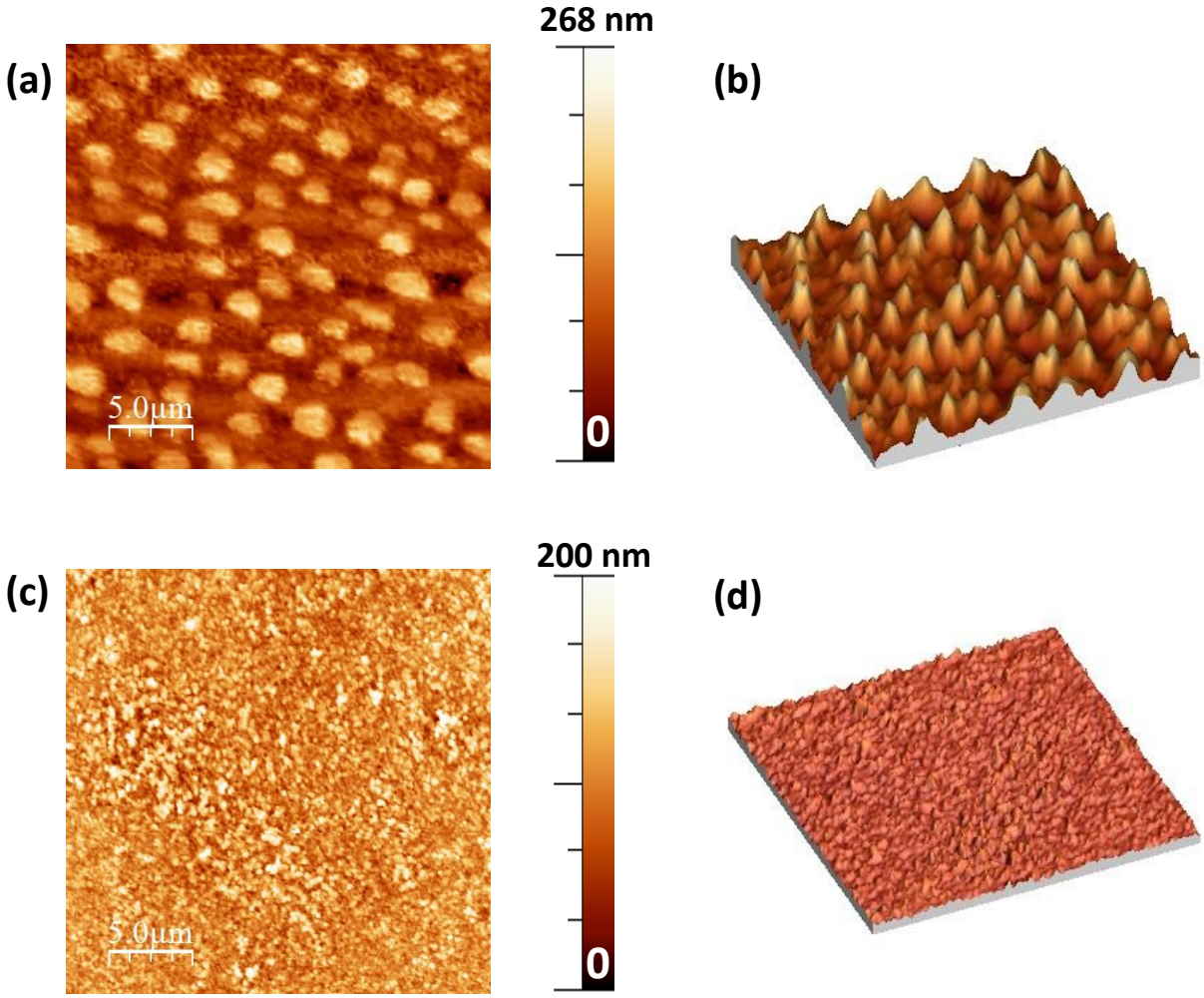

Figure S3. Atomic force microscope image of (a,b) textured film, (c,d) smooth film. The textured film shows the formation of micro-islands (MIs) where the average height of MIs is ~120 nm and an average distance of two such micro-island is around 3 μm. RMS roughness for perovskite films with and without micro-island structure was determined to be 40 nm and 21 nm respectively.

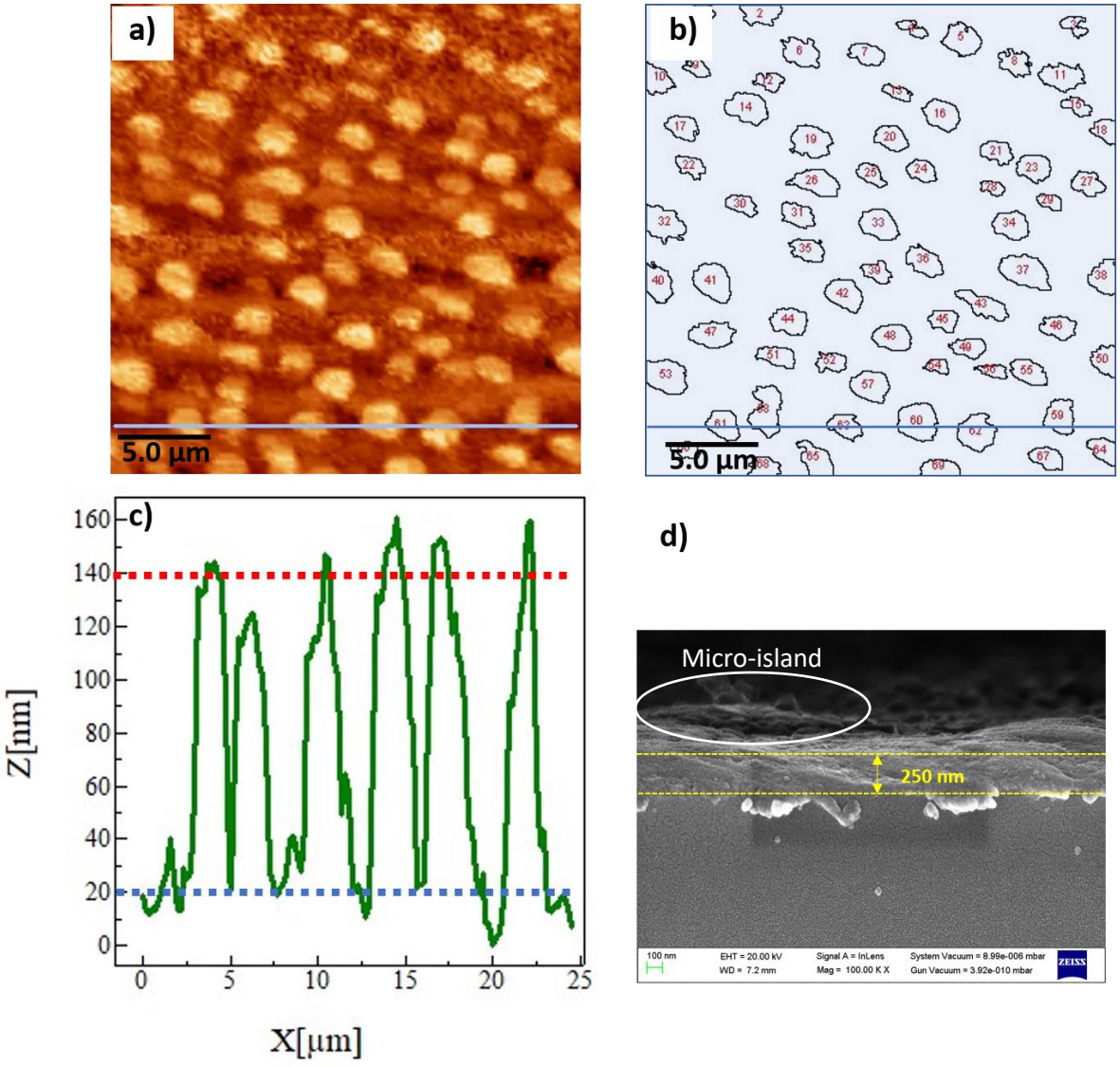

Figure S4. Figure (a) shows morphology of textured film captured by AFM (b) contour of the micro-islands (c) line profile of a textured morphology showing an average height for the micro-islands (d) Cross sectional FESEM image of anti-solvent treated film, scale bar is 500 nm.

Analysis of AFM image of textured film shows that the micro-islands cover 21.45% area of the film. The average height of the micro-islands was calculated to be 120 nm, if we consider these micro-islands to be semi-ellipsoidal in shape having an average height of 120 nm. Then, the textured films contribute additional 23.2 % surface area compared to a planer film, these semi-

ellipsoids over the film contribute only additional 6.8 % volume to the planer films, at the same time these micro-islands provide 750 % enhancement in PL intensity.

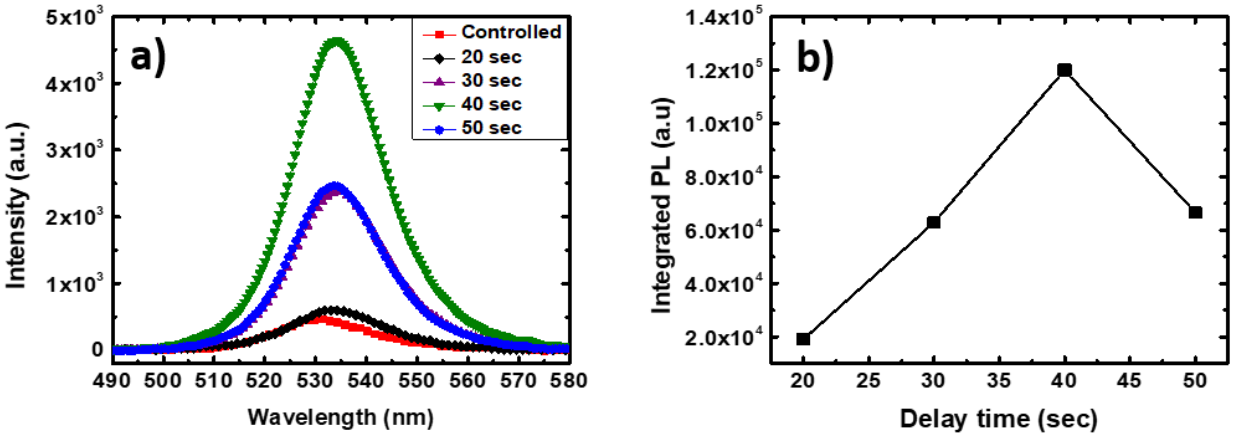

Figure S5. (a) Steady-state PL spectrum for different perovskite films optimized by antisolvent treatment at different delay times, integrated PL spectrum shows at least 7.5 times increase in PL intensity when micro-islands are present in the film compared to the planer films. At least 9.85 fold PL enhancement have been recorded for textured film compared to controlled films. (b) Integrated PL versus delay time for antisolvent treatment shows 40th second dripping time can be the optimum delay time.

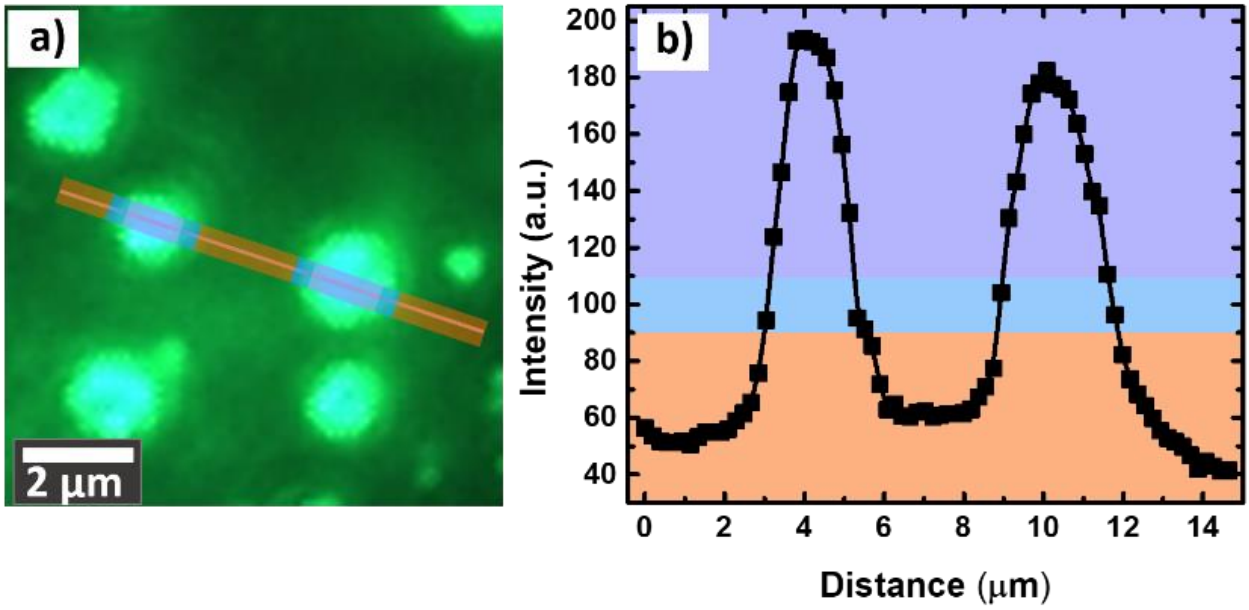

Figure S6. Line plot of PL intensity from perovskite film showing the lateral variation in PL intensity. The intensity values are grouped into three regions, intensity values below 90 gray scale value (GSV) are from the regions away from the micro-islands, whereas 90-110 GSV mark the boundary of the micro-island. Intensity values > 110 are from the micro-islands itself.

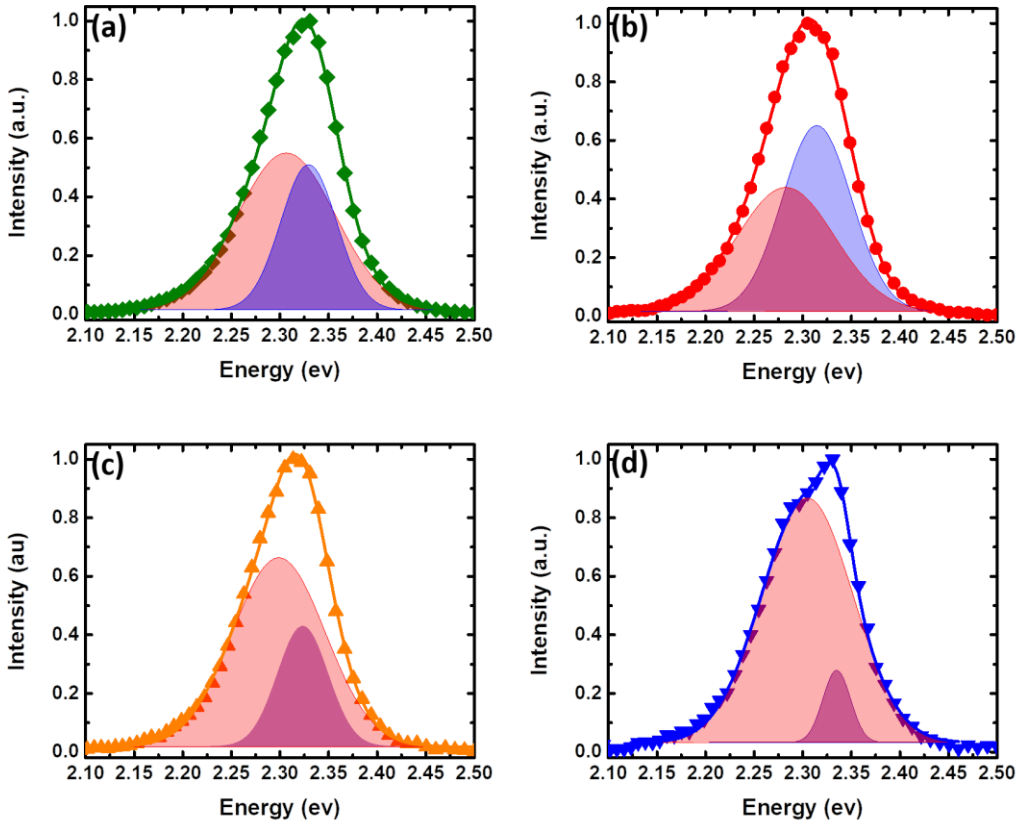

Figure S7. Analysis of PL spectrum from hyperspectral PL imaging. PL spectrum from different locations on textured-film is fitted with a superposition of two Gaussian functions. Shaded regions show the contributions of two emitters.

Hyperspectral PL imaging of controlled films showing that the micro-cubes are not emitting homogeneously, the emission from the edges of is approx. 3 times higher than the center of the cube although the QFLS at the brightest point is just 5 meV higher than the QFLS at the least bright point, which indicates that the intensity variation within the micro-cube could be because of out-coupling effect rather than the variations in trap density.

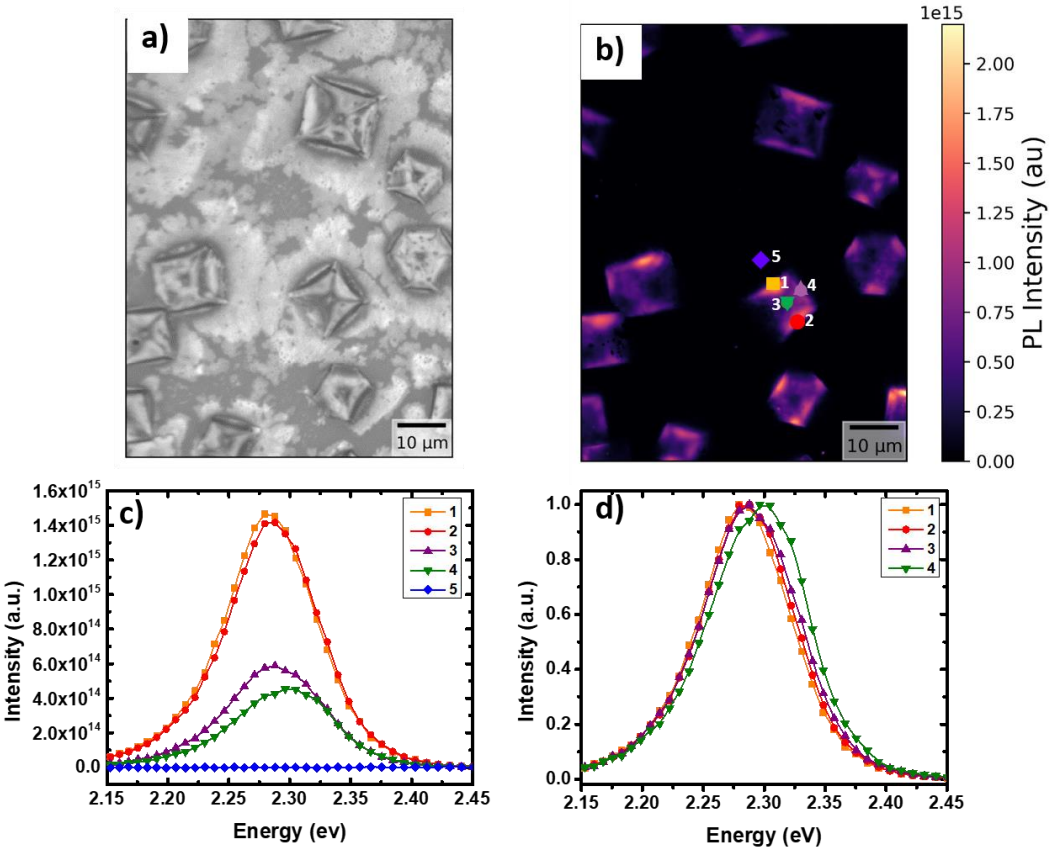

Figure S8. Hyperspectral PL imaging: correlated (a)transmission and (b) PL mode images taken by hyperspectral PL microscope (c) PL spectrum taken from different locations of the perovskite (d) Normalized PL spectrum showing ~12 meV distribution in the emission spectrum.

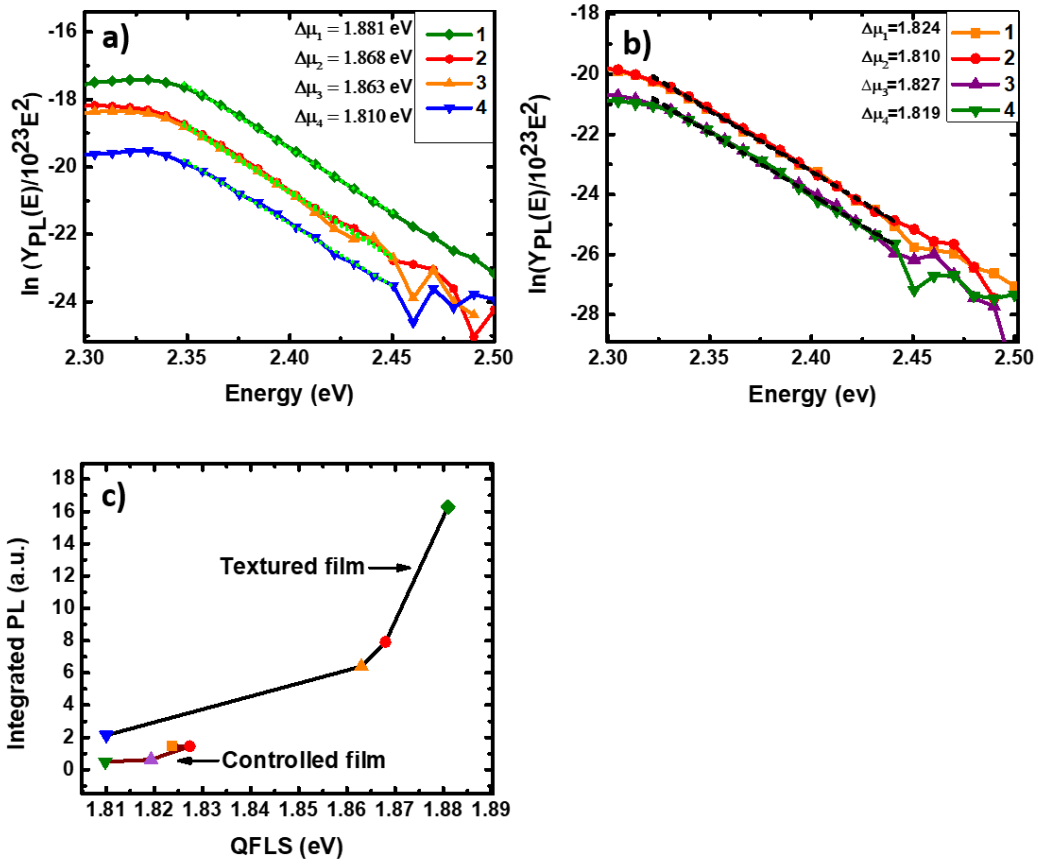

Figure S9. Calculation of quasi fermi level splitting (QFLS) in (a) anti-solvent treated (textured) film (b) controlled film using generalized Planck's law. (c) PL intensity versus QFLS showing small variations (~17 meV) within micro-cubes, whereas ~72 meV variation in anti-solvent treated film.

To verify that the instrument was properly calibrated to give the value of PL yield ($Y_{PL}(E)$) we have fitted $-ln\left(\frac{y_{p_l}(E)}{10^{23}E^2}\right)$ versus $\frac{h\nu}{kT}$ (Figure S10). According to Planck's generalized law[1] the linear fit is expected to give a value of slope which must approach unity.

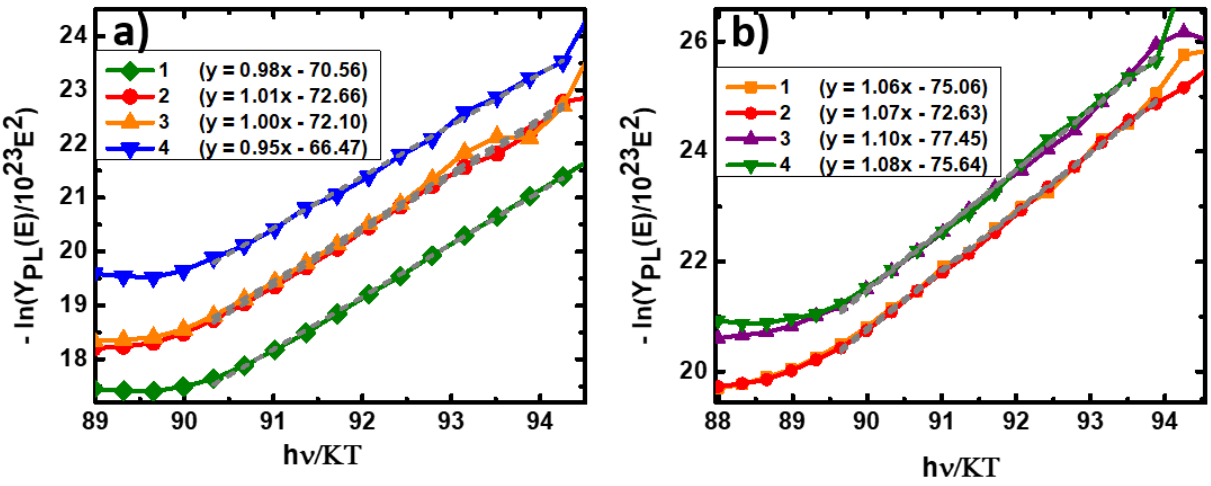

Figur S10. Fitting of $-\ln(Y_{PL}(E)/10^{23}E^2)$ versus $\hbar\omega/KT$. Fitting considers that the samples are maintained at room temperature (T=300 K). (a) fitting for texture film (b) fitting for controlled film.

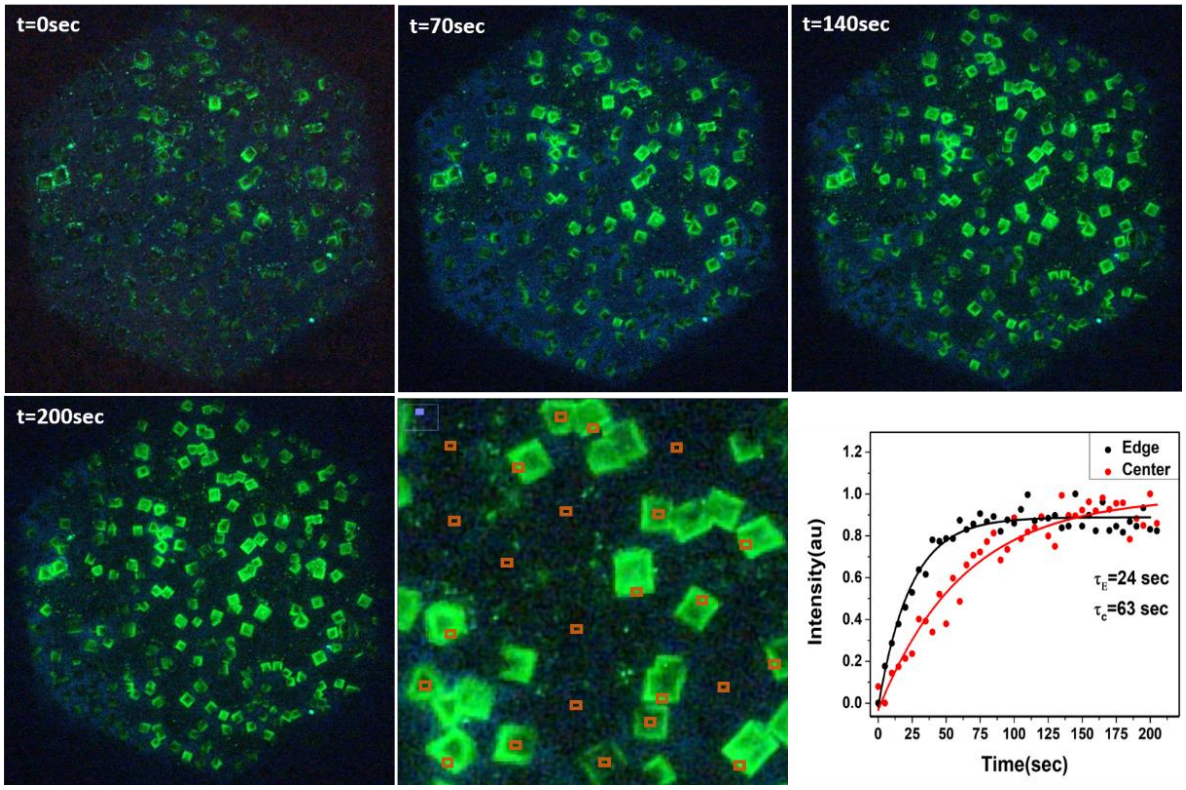

Figure S11. Photoluminescence enhancement of controlled film of microcubes at different time snap. Graphical representation of PL enhancement from the edges and the center of the microcube obtained from the multiple pixels of different microcubes.

The photoluminescence decay dynamics showed an initially fast component followed by a slow component for all three samples, (Figure S12). The fast component for controlled, smooth and textured films was were found to be 0.30 ns, 2.20 ns and 6.35 ns respectively, whereas the slow components for controlled, smooth and textured films were found to be 5.18 ns, 29.92 and 86.27 ns respectively. The fast PL decay component is usually associated with fast non-radiative decay pathways.[2] An increased average lifetime in textured film morphologies supports the enhancement of PL in textured film.

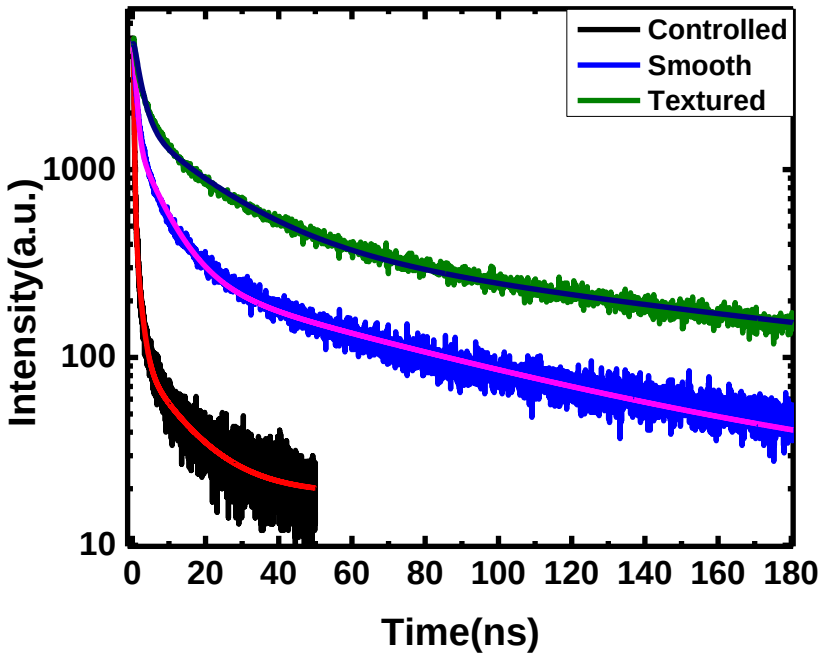

Figure S12. Transient PL decays for CH3NH3PbBr3 thin film, decay profiles for controlled, smooth and textured are fitted with a bi-exponential function.

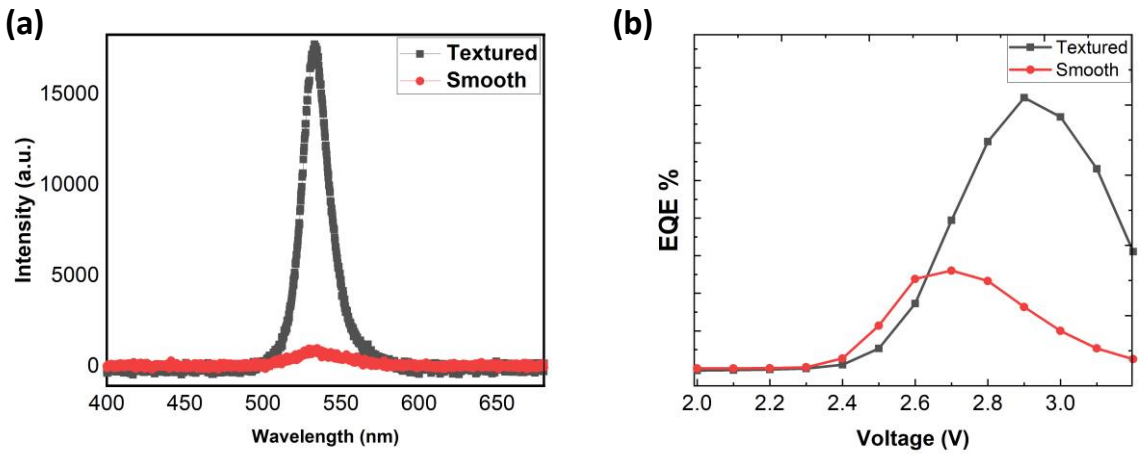

Figure S13. External quantum efficiency of smooth and textured perovskite film based PLEDs, show at least 2.7 times improvement when textured morphology is employed as emissive layer.

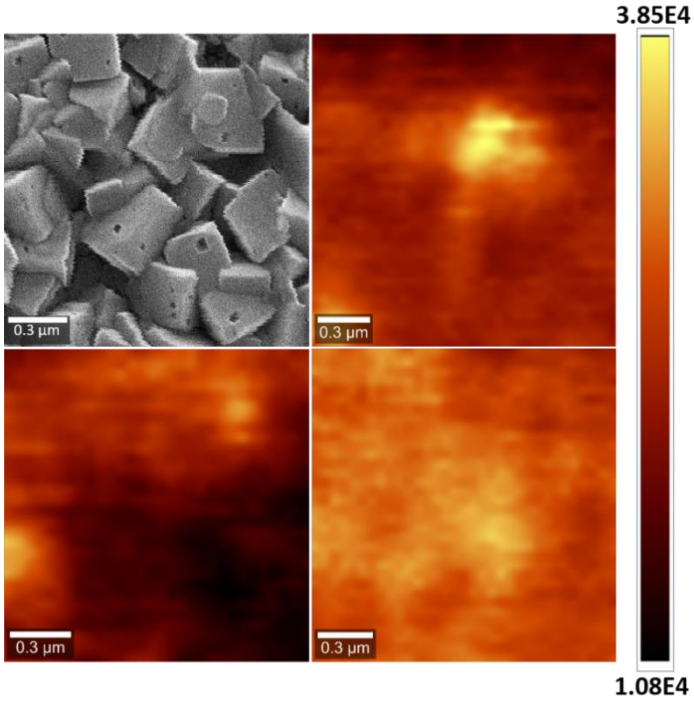

Figure S14. A typical film-area which is away from the micro-island site a) FESEM image showing presence of multi-grain structure (b-d) NSOM images of PL map for 3 different typical sample areas showing small variations in PL intensity from grain interior to grain boundary, which is an indication of smooth inter-grain diffusion of charge carriers in perovskite films.

In Figure S14 we have shown that the PL intensity variation at the scale of grain size is minor which is an indication of efficient inter-grain diffusion in smooth perovskite film. This efficient inter-grain diffusion may help the charge carriers to funnel to the non-radiative sites and decrease the PL intensity.

Table 1. Intensity versus QFLS for textured film.

Location	Integrated PL intensity	QFLS	
1	1.62E15	1.881	R(PL,QFLS) = 0.84
2	7.91E14	1.868	
3	6.40E14	1.863	
4	2.14E14	1.810	

Table 2. Intensity versus QFLS for controlled film.

Location	Integrated PL intensity	QFLS	
1	1.49E14	1.824	R(PL,QFLS) = 0.88
2	1.46E14	1.827	
3	6.23E13	1.819	
4	4.93E13	1.810	

Table 3: Time-resolved PL decay parameters of controlled and antisolvent treated (smooth and micro-island containing) perovskite films

	Controlled film		Smooth film		Micro-island film	
τ (ns)	τ_1 0.30	τ_2 5.18	τ_1 2.20	τ_2 29.92	τ_1 6.35	τ_2 86.27
B	B1 1.04	B2 0.04	B1 0.85	B2 0.15	B1 0.84	B2 0.18

References

(1) Abou-ras, D.; Kirchartz, T. *Edited by Physics of Solar Cells Thin Film Solar Cells Handbook of Photovoltaic Science and Engineering*; 2011.

(2) Shi, D.; Adinolfi, V.; Comin, R.; Yuan, M.; Alarousu, E.; Buin, A.; Chen, Y.; Hoogland, S.; Rothenberger, A.; Katsiev, K.; Losovyj, Y.; Zhang, X.; Dowben, P. A.; Mohammed, O. F.; Sargent, E. H.; Bakr, O. M. Low Trap-State Density and Long Carrier Diffusion in Organolead Trihalide Perovskite Single Crystals. *Science (80-.).* **2015**, *347* (6221), 519–522. https://doi.org/10.1126/science.aaa2725.